High energy-resolution measurements of x-ray into ultraviolet parametric down-conversion with an x-ray tube source

D. Borodin,[a)] S. Levy,[a)] and S. Shwartz[b)]
Physics Department and Institute of Nanotechnology, Bar Ilan University, Ramat Gan 52900, Israel

We describe high energy-resolution measurements of parametric down-conversion of x-rays into ultraviolet radiation using a standard laboratory x-ray tube source with very minor modifications. We measure the effect in diamond and in lithium fluoride crystals in the ultraviolet range from 30 eV to 65 eV. We show that the effect depends strongly on the fluorine L_I edge at 37 eV and on the K edge of the lithium at 55 eV. The comparison with theory reveals that the classical model that was previously used for the description of the effect agrees with the experimental results in diamond. However, the discrepancies of the model with the experimental results in lithium fluoride are prominent. *Published by AIP Publishing.* [http://dx.doi.org/10.1063/1.4979413]

Parametric down-conversion (PDC) of x-rays into ultraviolet (UV) radiation is a second order nonlinear process in which a pump photon interacts with the vacuum field to generate an x-ray photon and a UV photon. The x-ray photon is usually denoted as the signal photon and the UV photon is called the idler photon. Since the absorption length in the UV range is much shorter than the thickness of most samples, in a typical experiment, only the signal photons are measured. Due to energy and momentum conservations, the photon energies and the angles of propagation of the generated photons are correlated. Since the signal and idler photons are generated simultaneously at the same position, the rate of the signal photons depends on both the x-ray and UV properties of the material. Consequently, it is possible to retrieve the information on the UV interactions from the measurements of the x-ray photons only. Since these interactions depend on the charge distribution and on the binding energies of the valence electrons, it has been proposed that PDC of x-rays into UV can be used as a powerful tool for the studies of properties of the valence electrons in crystals.[1] Indeed, several experiments have advanced these applications.[2–6] However, a practical application requires an energy resolution of a few eV or less. This requirement has been satisfied at synchrotron facilities.[4,6] Yet, it is not obvious that it can be achieved with laboratory systems. This is because (1) the low efficiency leads to very low count rates and to the requirement of a very careful design of the experiment to avoid signal losses and (2) the short distances between the sample and the analyzer and between the analyzer and the detector as imposed by the enclosure of the laboratory systems introduce a major challenge in separating the signal from the background. In the only one experimental demonstration with an x-ray tube source, the energy resolution was limited by the energy resolution of the detector, which is larger than 125 eV.[2]

Here, we describe experiments demonstrating the ability to perform high energy-resolution measurements of

x-rays into UV PDC with laboratory x-ray systems. We overcome the low count rate challenge by using a silicon drift detector with a dark count rate of less than 1 count per 1000 s. We increase the signal-to-noise-ratio by inserting narrow slits before and after the Ge(220) 2-bounce channel-cut analyzer and by carefully aligning their positions with respect to the center of the beam. We measure the effect in diamond and in LiF crystals in the UV range of between 30 eV and 65 eV with an energy resolution of a few eV, which is comparable to the resolution reported with synchrotron experiments. In this regime, we measure the effect in LiF near the fluorine L_I edge at 37 eV and near the K edge of the lithium at 55 eV and show that the effect is atomic selective.

The nonlinearity supporting x-ray PDC is originated from the Lorentz force and spatial distribution of the electron density.[7,8] It was shown that far from resonances, the linear optical response and nonlinear second order optical response are related via the following expression:[5,7,8]

$$\chi_G^{(2)}(\omega_p = \omega_s + \omega_i) = \frac{e}{2\omega_s mc} \times \chi_G^{(1)}(\omega_i) \times \theta_{psi}, \quad (1)$$

where $\chi_G^{(n)}(\omega_j)$ is n-th order of the G-th Fourier component of the optical susceptibility at the j-th frequency. The indices p, s, and i represent the pump, signal, and idler, respectively, θ_{psi} is the polarization factor, e and m are the electron charge and mass, respectively, and c is the speed of light. The generated photons satisfy energy and momentum conservation (phase matching). The energy conservation law can be written as $\hbar\omega_p = \hbar\omega_s + \hbar\omega_i$. Since x-ray wavelengths are comparable to the interatomic distances, the momentum conservation is achieved by using the reciprocal lattice vector $\vec{G}$[7] and the phase matching can be expressed as

$$\vec{k}_p + \vec{G} = \vec{k}_s + \vec{k}_i, \quad (2)$$

where $\vec{k}$ has a meaning of a wave-vector of the pump, signal, and the idler photons, respectively. The phase-matching diagram is shown in Fig. 1(a). Here, θ_p, θ_s, and θ_i are the angles with respect to the atomic planes of the pump, signal, and idler, respectively.

---

a)D. Borodin and S. Levy contributed equally to this work.
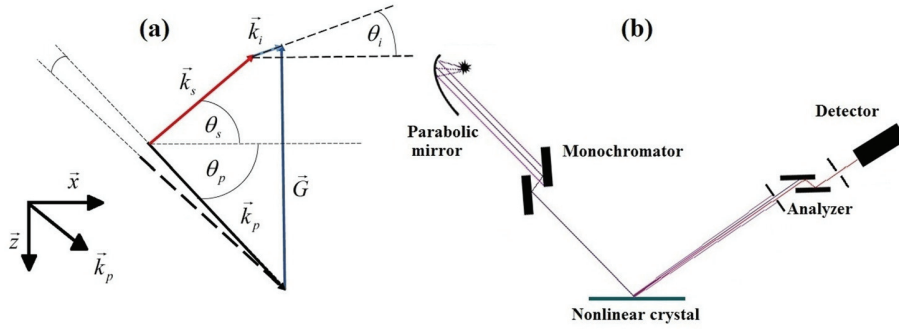b)Author to whom correspondence should be addressed. Electronic mail: sharon.shwartz@biu.ac.il.

FIG. 1. (a) Phase-matching scheme. The vectors $\vec{k}_p$, $\vec{k}_s$, and $\vec{k}_i$ are the k-vectors of the pump, signal, and idler, respectively. $\vec{G}$ is the reciprocal lattice vector. Dashed line indicates Bragg condition. (b) Experimental setup.

Since the expected signal is very weak, it is worth discussing the possible sources for noise. The main source is the tail of the Bragg scattering. This is because the efficiency of the elastic scattering is about 8 orders of magnitude higher than the efficiency of PDC. Indeed, even after the analyzer crystal we find non-negligible photons from the Bragg tail. Fortunately, the Bragg rocking curve is narrower than the PDC rocking curve and thus we can distinguish between Bragg and PDC by scanning the angle of the source relative to the Bragg angle. The next potential noise is Compton scattering. We estimate that the Compton shifts in our experiments are about 95 eV and 150 eV for the diamond and the LiF experiments, respectively. Since these energies are far from the idler energies we considered, the analyzer crystal filters them out very efficiently. Another source for noise is x-ray Raman scattering, but far from resonances this effect is very weak.

We use a Rigaku Smartlab 9 kW x-ray diffractometer (XRD) with a rotating anode. The copper Kα1 beam is collimated and monochromatized by a parabolic multilayer mirror and a Ge(220) channel-cut monochromator. The scheme of the experimental setup is shown in Fig. 1(b). We calibrate the analyzer in accord with copper Kα1 and Kα2 lines and with bremsstrahlung. We estimate that the energy resolution of the analyzer is about 3 eV. The incident flux is about 4×10^8 photons/s after the monochromator.

We begin by finding the Bragg reflection and measuring the rocking curve with the analyzer tuned to the copper Kα1 line. Next, we move the source and the detector to the PDC phase-matching angles. The analyzer is set to the photon energy of the signal photon. We use slits before and after the analyzer to select a narrow angle range and to filter out residual elastic photons. We first scan over the angle of the source (pump) with respect to the crystal. We optimize the signal and signal-to-noise-ratio by scanning over the detector arm and the analyzer angle. We use the (220) reflection for the measurements in diamond and the (400) reflection in the measurements in LiF.

Fig. 2 shows the signal count rate as a function of the deviation of the pump angle from the phase-matching angle, which we denote as $\Delta\theta_p$. The solid lines are the theoretical calculations where we use the nonlinear susceptibility of Eq. (1)[7,8] together with the coupled wave equations for the signal and idler operators in the slowly varying envelope approximation.[9] Fig. 2(a) depicts $\Delta\theta_p$ scans for the diamond crystal. The idler energy is 30 eV, and the offset of the source is 2 mrad from the Bragg angle. It is clear that the PDC peak is

shifted from the exact phase-matching angle. The same shift is shown in the theoretical calculations as well. The two sharp peaks at $-0.11°$ and at zero are due to the residual Bragg diffraction. The left narrow peak matches the offset from the Bragg angle so it originates from the Bragg tail. In addition, since the analyzer crystal is coupled to the detector arm, when the detector arm is rotated, the angle of analyzer crystal with respect to the scattered beam is shifted and a second narrow peak appears. In Figs. 2(b) and 2(c), the measurements for the LiF crystal for the two possible solutions of Eq. (2) are shown. The detector angles with respect to the Bragg angle are $0.3184°$ and $-0.2185°$. The idler energy is 40 eV and the offset from the Bragg angle is 5 mrad. We find that the calculated count rates are smaller by a factor of about 5 from the measured count rates and that the measured rocking curves are broader than the theoretical prediction. The discrepancies in the widths can be explained by the mosaic spread of the LiF crystal. To reconcile between the theoretical and measured efficiencies, a quantum model, which considers local field correction for the nonlinearity, is most likely required. We emphasize that both the theoretical calculations and the experimental measurements show the shift of the maximum of the PDC effect from the exact phase-matching angle. The shift depends on the phase-matching equation solution and on the offset from Bragg condition. Interestingly, the measured efficiencies of the PDC for the two solutions of Eq. (2) [shown in Figs. 2(b) and 2(c)] are not equal in agreement with the theoretical
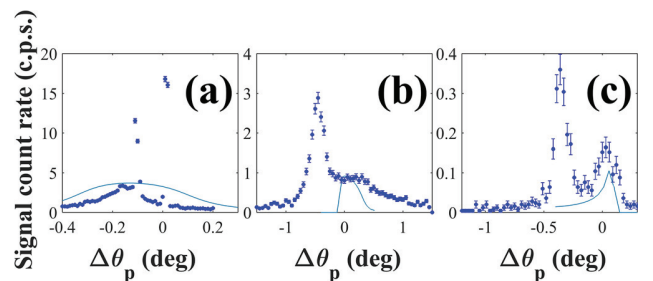

FIG. 2. Signal count rate as a function of the deviation from phase matching for (a) diamond and (b) and (c) LiF. (b) and (c) correspond to two solutions of the phase-matching equation, with a larger and a smaller angle with respect to the Bragg angle, respectively. The idler energies are 30 and 40 eV for diamond and LiF measurements, respectively. The zero on the abscissa corresponds to the phase-matching condition. Dots with error bars are the experimental measurements and the solid lines are theoretical simulations. The PDC curves are the board curves. The strong sharp peaks are due to the Bragg reflection. The theoretical calculations for LiF are multiplied by a factor of 5. The vertical error bars indicate counting statistics.
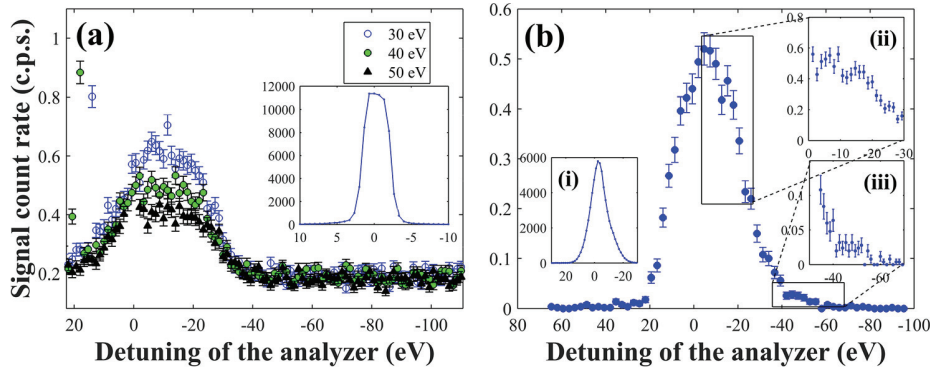
FIG. 3. Signal count rate versus the analyzer detuning from the pump energy for various phase-matching conditions of (a) diamond and (b) LiF. The zero on the abscissa axis is the pump energy. In (a) the legend indicates the idler energy and the offset from the Bragg condition is 2 mrad. The inset shows the scan at the Bragg condition. (b) The source and the detector are at angles that correspond to phase matching at an idler energy of 40 eV and offset from the Bragg angle of 5 mrad. Inset (i) shows the scan at the Bragg condition. Insets (ii) and (iii) show scans around the 2p excitations and around the phase-matching region, respectively. The vertical error bars indicate the counting statistics.

calculations. The strong peaks on the left of the PDC curves also originate from the Bragg tail. The position matches the offset from the Bragg angle considering the mosaic spread of the crystal and rather broad (about 0.1°) rocking curve of the Bragg reflection.

To understand the shift in the curve with respect to the phase matching, we recall that a large number of vacuum modes contribute to the PDC effect and that there is a one-to-one correspondence between the photon energies and the angles imposed by the phase-matching condition. Since the detector has a finite aperture, modes (including modes with $\Delta k_z \neq 0$) at various photon energies and angles are collected. The measured count rate is the sum of all the possible modes that are limited by the acceptance angle of the detector, by the bandwidth of the analyzer, and by the boundary conditions. In addition, since the nonlinearity increases as the idler photon energy decreases, the contributions of the lower photon energy modes are larger. This leads to the asymmetric line shape and to a shift in the rocking curve. The difference between the efficiencies at the different phase matching solutions is because the angles of the idler photon with regard to the crystal surface are different for the two solutions.

Fig. 3(a) shows the analyzer scans where the angles of the source and the detector are at the phase-matching angles corresponding to idler photon energies of 30 eV (empty circles), 40 eV (green circles), and 50 eV (black triangles). The corresponding shifts of the detector from the Bragg angle are 0.12°, 0.18°, and 0.23°, respectively. The size of the slit before the analyzer is 0.1 mm. Except from the sharp and narrow elastic peak that corresponds to the residual elastic scattering, we see a broad peak at each of the curves. The energy of this peak corresponds not to the selected idler photon energy but to the binding energy of 2p electrons in diamond at 11.3 eV.[10] At this energy, the PDC effect is much stronger because of the resonant enhancement of the nonlinear susceptibility.[6] The curves of the analyzer scans are broad because of numerous vacuum fluctuation modes that contribute to the count rate. The heights of curves decrease as the idler energies increase as expected. We note that the elastic peak is shifted from its position when the angles of

the source and the detector satisfy the Bragg condition. This is because the analyzer crystal and the sample have the same scattering planes. Fig. 3(b) shows the analyzer scan for the LiF crystal for the phase-matching conditions corresponding to the idler energy at 40 eV. The main peak is around 5 eV and corresponds to the 2s electrons of the lithium atoms.[10] Inset (ii) reveals a bump near 17 eV, which corresponds to the 2p electrons of the fluorine atoms.[10] Finally, inset (iii) shows a hump that corresponds to the signal for the chosen idler energy at 40 eV.

Another interesting phenomenon occurs when the idler energy is chosen to be close to absorption edges[6] as shown in Fig. 4, which describes the spectral dependence of the PDC in the LiF crystal. The size of the slit before the analyzer in these measurements is 1 mm. Each of the points in this figure represents the peak of the rocking curve at the idler energy of the horizontal axis. We clearly see a strong peak near the L_I absorption edge (2s level) of the fluorine atoms at 37 eV. The peak is shifted to the higher energies in agreement with previous observations.[11] The authors of Ref. 6 suggest that the resonant behavior of the PDC occurs when the atomic structure factor f_I becomes negative. In the current case, the tabulated values of f_I for fluorine are
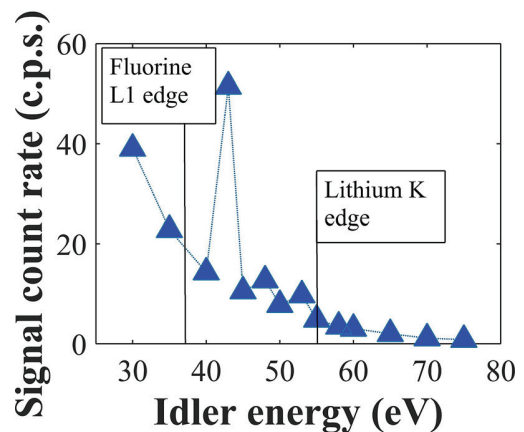

FIG. 4. Spectral dependence of the efficiency of PDC process in LiF. The vertical black solid lines correspond to the L_I edge of the neutral fluorine atom and the K edge of the neutral lithium atom.

positive.[12] However, it should be noted that those tabulate values are not accurate in the UV range. In particular, they do not show any resonance in the spectral dependence of f_2 of the fluorine near 37 eV in contrast to previous experimental and theoretical reports.[11,13,14] Therefore, the comparison with theory requires more accurate theoretical calculations.

In conclusion, we described experimental results showing the effect of x-rays into UV PDC with an energy resolution of a few eV obtained by using a standard laboratory source. We presented data for diamond and LiF samples. Our results suggest that the classical model for the nonlinearity is adequate for the description of PDC of x-rays into UV far from resonances in diamond in agreement with the previous synchrotron work.[3–6] For LiF, the predicted efficiency is about five times weaker than the measured efficiency and the model does not show any resonance near 43 eV in contrast to the experiments. Hence, a different model for nonlinearity should be considered. We found that the efficiency of the effect varies rapidly near the L_I edge of fluorine and the K edge of the lithium and conclude that it is therefore atomic selective. The relatively simple setup of the experiments we described and the availability of commercial detectors with very low dark count noise open a possibility for broader studies on electronic properties of materials using x-rays into UV PDC with low brightness systems. The observation of the effect with low flux advances the possibility for applications in spectroscopy of samples with very low radiation damage threshold such as biological samples.

[1] I. Freund, Chem. Phys. Lett. **12**, 583 (1972).
[2] H. Danino and I. Freund, Phys. Rev. Lett. **46**, 1127 (1981).
[3] K. Tamasaku and T. Ishikawa, Phys. Rev. Lett. **98**, 244801 (2007).
[4] K. Tamasaku, K. Sawada, and T. Ishikawa, Phys. Rev. Lett. **103**, 254801 (2009).
[5] K. Tamasaku, K. Sawada, E. Nishibori, and T. Ishikawa, Nat. Phys. **7**(9), 705–708 (2011).
[6] B. Barbiellini, Y. Joly, and K. Tamasaku, Phys. Rev. B **92**, 155119 (2015).
[7] I. Freund and B. F. Levine, Phys. Rev. Lett. **23**, 854 (1969).
[8] P. M. Eisenberger and S. L. McCall, Phys. Rev. Lett. **26**, 684 (1971).
[9] S. Shwartz, R. N. Coffee, J. M. Feldkamp, Y. Feng, J. B. Hastings, G. Y. Yin, and S. E. Harris, Phys. Rev. Lett. **109**, 013602 (2012).
[10] See http://www.chemistry.uoguelph.ca/educmat/atomdata/bindener/elecbind.htm for tabulated values of electron binding energies; accessed 2 February 2017.
[11] V. Mauchamp, P. Moreau, G. Ouvard, and F. Boucher, Phys. Rev. B **77**, 045117 (2008).
[12] See http://henke.lbl.gov/optical_constants/asf.html for the atomic scattering factor data; accessed 18 January 2017.
[13] P. Abbamonte, T. Graber, J. P. Reed, S. Smadici, C.-L. Yeh, A. Shukla, J.-P. Rueff, and W. Ku, Proc. Natl. Acad. Sci. U.S.A. **105**, 12159 (2008).
[14] A. Zunger and A. J. Freeman, Phys. Rev. B **16**, 2901 (1977).